Al-Nahrain Journal for Engineering Sciences **NJES** 27(4)477-484, 2024
http://doi.org/10.29194/NJES.27040477

The Assessment of Spinal Alignment Based on a Computer-Assisted Electromechanical Device

Esraa K. Mahan[1]*, Aseel Ghazwan[2], Luay Asaad Mahmood [3]

Authors affiliations:
1*) Department of Biomedical Engineering, Al-Nahrain University, Baghdad, Iraq
esraa.khalifa.msc2023@ced.nahrainuniv.edu.iq

2) Department of Biomedical Engineering, Al-Nahrain University, Baghdad, Iraq
aseel_ghazwan@yahoo.com

3) Department of Orthopedics and traumatology, Medical College, University of Anbar, Anbar, Iraq
amahmood@uoanbar.edu.iq

Paper History:

Received: 26th Jun. 2024

Revised: 4th May 2024

Accepted: 27th Sep. 2024

Abstract

Spinal alignment examination procedures are frequently employed to assess spinal deformities. The spine plays a crucial role in maintaining the biomechanical functionality of the skeletal system. It protects the spinal cord and facilitates movement, among other vital functions. Various methods, including radiography and non-invasive techniques such as goniometer, inclinometer and kyphometer, have been employed to assess spine alignment qualitatively. Nevertheless, these methods are characterized by a high radiation dose and require significant time.

Consequently, this study aimed to develop and create a spinal mouse (SM), which is portable, user-friendly, radiation-free computer-assisted electromechanical device to assess spinal deformities in the sagittal plane by measuring the angle between two vertebrae in the segmental and global thoracic and lumbar regions, as well as the spine's length. This study showed the significance of the technique in assessing spinal alignment. The angle between the two vertebrae was recorded using the MPU-6050 sensor, and the spine's length was measured using the rotary encoder. Afterwards, the data was sent to a computer using a Bluetooth module link once the Arduino Nano microcontroller had processed it.

Three examiners passed the device on the volunteer's back, starting from C7 to S1, after palpating the area to identify it with a cosmetic pen, allowed the proposed system to be used on five healthy adult subjects to assess their standing posture in the sagittal plane, specifically in the upright, flexion, and extension positions to assess intra- and inter-rater reliability.

The suggested SM device assessed total sagittal spinal alignment in the thoracic and lumbar regions with good intra- and inter-rater reliability. This apparatus also worked well for segmental lumbar extension measures amongst examiners. The proposed device was simple, portable, and affordable, allowing for quick and accurate sagittal spinal alignment evaluation. It speeds up clinical examination and is safe for patients, resulting in precise diagnosis.

Keywords: SM, Thoracic Segment Angle, Lumber Segment Angle, Sagittal Spinal Alignment, Spinal Length.

تقييم محاذاة العمود الفقري بناءً على التصنيف الوضعي للعمود الفقري السهمي المعدل

اسراء خليفة محان، اسيل غزوان، لؤي أسعد محمود

الخلاصة:

تُستخدم إجراءات فحص محاذاة العمود الفقري بشكل متكرر لتقييم تشوهات العمود الفقري. يلعب العمود الفقري دورًا حاسمًا في الحفاظ على الوظيفة الميكانيكية الحيوية للجهاز الهيكلي في جسم الإنسان. فهو يحمي الحبل الشوكي ويسهل الحركة، من بين الوظائف الحيوية الأخرى. تم استخدام طرق مختلفة، بما في ذلك التصوير الشعاعي والتقنيات غير الجراحية مثل kyphometer, goniometer, and inclinometer ، لتقييم محاذاة العمود الفقري نوعياً. ومع ذلك، تتميز هذه الطرق بجرعة إشعاعية عالية وتتطلب وقتًا كبيرًا.

NJES is an **open access Journal** with **ISSN 2521-9154** and **eISSN 2521-9162**

وبالتالي، تهدف هذه الدراسة إلى تطوير وإنشاء جهاز كهروميكانيكي محمول وسهل الاستخدام وخالي من الإشعاع ومدعم بالكمبيوتر لتقييم تشوهات العمود الفقري. الغرض من هذا الجهاز المقترح هو تقييم محاذاة العمود الفقري السهمي عن طريق قياس الزاوية بين فقرتين في المناطق الصدرية والقطنية القطاعية والعالمية، بالإضافة إلى طول العمود الفقري. وأظهرت هذه الدراسة أهمية هذه التقنية في تقييم محاذاة العمود الفقري. تم تسجيل الزاوية بين الفقرتين باستخدام جهاز الاستشعار MPU-6050، وتم قياس طول العمود الفقري باستخدام جهاز التشفير الدوار. بعد ذلك، تم إرسال البيانات إلى جهاز كمبيوتر باستخدام رابط وحدة Bluetooth بمجرد قيام وحدة التحكم الدقيقة Arduino Nano بمعالجتها. قام ثلاثة فاحصين بتمرير الجهاز على ظهر المتطوع، بدءًا من C7 إلى S1 ، بعد تحسس المنطقة للتعرف عليها باستخدام قلم تجميلي، مما سمح باستخدام النظام المقترح على خمسة أشخاص بالغين أصحاء لتقييم وضعية وقوفهم في المستوى السهمي. على وجه التحديد في الوضع المستقيم والانحناء والتمدد لتقييم الموثوقية داخل وبين المقيم.

قام جهاز SM المقترح بتقييم المحاذاة الإجمالية للعمود الفقري السهمي في منحنى الفقرات الصدرية والقطنية مع موثوقية جيدة داخل وبين الفاحصين. لقد نجح هذا الجهاز أيضًا بشكل جيد في قياسات التمديد في منحنى الفقرات القطنية بين الفاحصين. كان الجهاز المقترح محمولًا وبسيطا وبسعر معقول، مما يسمح بتقييم محاذاة العمود الفقري السهمي بسرعة ودقة. إنه يسرع الفحص السريري وهو آمن للمرضى، مما يؤدي إلى تشخيص دقيق.

في المستقبل، يمكن تحسين الجهاز المقترح لتقييم تشوه العمود الفقري في المستوى الأمامي في مواضع مختلفة. بالإضافة إلى ذلك، فإنه يحسب نطاق الحركة. من الممكن تحسين برنامج الجهاز المقترح للسماح بنقل البيانات وتحميلها من أي مكان.

1. Introduction

The spinal column serves as the primary axis of the skeletal system in the human body. The structure is composed of five sections arranged in a cephalocaudal sequence: cervical, thoracic, lumbar, sacral, and coccygeal[1]. The spinal column consists of 33 vertebrae, which are classified as seven cervical vertebrae, twelve thoracic vertebrae, five lumbar vertebrae, five sacral vertebrae, and four coccygeal vertebrae. The cervical, thoracic, and lumbar parts of the spine allow each vertebra to move with respect to the vertebrae next to it. The spinal cord is shielded from external damage by the vertebral column, which encloses it within the vertebral canal [2].

Spinal alignment is adversely affected by several factors, such as age, body mass index (BMI), gender, obesity, prolonged use of smartphones/computers, hyper-kyphosis, incorrect posture, and leftward tilt of the spine. These factors enhance the probability of having back discomfort and lead to spine deformity [3-12]. In addition, other biological conditions can affect spinal health, such as urine incontinence (UI) [13] and locomotor syndrome (LS) [14, 15], which have an impact on the sagittal spinal curvature and its mobility.

Different methods have been introduced to examine the alignment and mobility of the spinal column, as well as to measure the curvatures in individuals with spinal abnormalities. Imaging techniques are commonly employed, and they can be conducted using various methods such as x-ray, CT, and MRI [16]. However, it is important to recognize that this method carries the risk of prolonged exposure to radiation, for x-ray and CT methods, especially when multiple examinations are needed to assess the patient's spinal status [17], and magnetic artefacts [18] for the latter. Consequently, numerous non-invasive external techniques have been introduced, including goniometers [19], kyphometers [20], digital inclinometers [21], etc. These techniques either have low reliability and validity or require a significant amount of time [22].

The SM, created by Idiag in Switzerland, is a portable computerized electromechanical device that records measurements of spinal curvature. Furthermore, the SM was employed to evaluate spinal movement. In 1994, a research article was published by Dr. Seichert and Prof. Senn from the Ludwig Maximilian University of Munich, Germany. The article laid the foundation for the concept of a device specifically created to record the surface of the spine. This university houses the Clinic of Physical Medicine and Rehabilitation. The SM (Idiag M360) prototype was initially created in collaboration with Idiag AG, a Swiss business that specializes in software development. Idiag AG facilitated the initial introduction of the Idiag M360 devices to the Swiss market in 1999 [23].

Multiple investigations have examined the dependability and accuracy of the SM device for people who do not report any discomfort. Post and Leferink [24] conducted a study that included 111 subjects to assess the interrater reliability of a global and segmental range of motion (ROM) for spinal flexion and extension on the same day. The reliability of global flexion and extension was found to be excellent, with intra-class correlation coefficients (ICCs) of 0.95 and 0.92, respectively. However, there was poor agreement (kappa= 0.22) in determining when segmental flexion and extension values deviated from the range of normalized values provided by the computerized system [24]. While the SM device has shown consistently good reliability for assessing global

NJES is an **open access Journal** with **ISSN 2521-9154** and **eISSN 2521-9162**

spinal ROM, there is a broad range of reported reliability when it comes to determining segmental spinal ROM. Mannion et al. [25] found that the reliability of segmental flexion varied from poor to good between different days and between different raters. The reliability values ranged from 0.39 to 0.90 for intra-rater reliability and from 0.28 to 0.81 for inter-rater reliability. Zafereo et al. [26] conducted a study to analyze the reliability of a spinal ROM evaluation using an SM device. The study included 20 persons with low back pain (LBP) and 20 adults without LBP who were matched in terms of age and sex. The researchers examined both the intra-rater reliability on the same day and the inter-rater reliability. The study found that the ICCs for global ROM assessment were high, ranging from 0.76 to 0.96 for intra-rater reliability and from 0.77 to 0.93 for inter-rater reliability [26].

There is a high demand for SM in order to do a qualitative study of spine morphology. Nevertheless, the products now offered in the market are costly and lack accessibility. Consequently, this study aimed to create, produce, and enhance the SM using readily accessible components and materials at a reasonable price while also distinguishing it from the existing market device that incorporates three sensors. Each sensor measures the axis in the x, y, and z directions. Instead, this device utilizes a gyro sensor that accurately measures three axes, resulting in a reduction in parts, size, and weight; this allows for a cost-effective evaluation of spinal curvature, provides a visual representation of spine alignment, and enables precise estimation of clinical indicators for spinal deformities.

2. Materials and methods

2.1. Design

In the proposed system, the SM device will be utilized to calculate the variables that ascertain the degree of spinal deformity and assess the spine's alignment. The factors involve:

a) Evaluating the angle between two vertebrae.
b) Measuring the angle in the thoracic and lumbar regions.
c) Determining the length of the spine.

Afterwards, a thorough explanation will be given. The SM is fitted with accelerometers that gauge the separation between segments and the alteration in inclination of spinous processes as the device is rolled along the spine, namely from C7 to S1 [26]. In order to guarantee the exact positioning of the vertebrae and the correct calculation of inclination angles along the X, Y, and Z axes, the circuit design for this experiment incorporated two unique categories of sensors. An angle is the quantification of the rotational displacement of an item around a stationary point on a central axis, and it may be determined using the gyroscope sensor. The sensor data is transmitted to the Arduino Nano microcontroller using the I2C protocol and subsequently analyzed using a dedicated filter.

The gyroscope sensor signal was processed in real time on the Arduino Nano microcontroller using a moving average filter, which is a simple low-pass filter. A process of iterative experimentation achieves optimal window size selection. The proposed solution uses a window size of 10 samples to create a moving average filter using the Arduino Nano microcontroller. The purpose of this filter is to eradicate the time delay between the filter's input and output signals [27].

Before being sent to a computer using a Bluetooth module, the data undergoes processing to minimize high-frequency interference. The rotary encoder has been used to measure the position of the vertebrae. The operational basis of the rotary encoder involves the transmission of light through an aperture to a photodiode located on one side of the disk. A light beam is detected by a photodetector located on the opposite side of the disk.

The photodiode produces a waveform that is directly proportional to the intensity of the incoming light and exhibits an almost sinusoidal shape. A Schmitt Trigger is employed to convert the sinusoidal waveform into a square waveform [28]. The resulting digital signal is then passed to the Arduino Nano microcontroller for processing and subsequently sent to a PC via a Bluetooth module.

The circuit components were interconnected to ensure that each one fulfilled its designated function. The microcontroller has been successfully connected to all of its components. Fig. 1 illustrates the main hardware components. The software was integrated with the hardware components of the entire system for functioning.

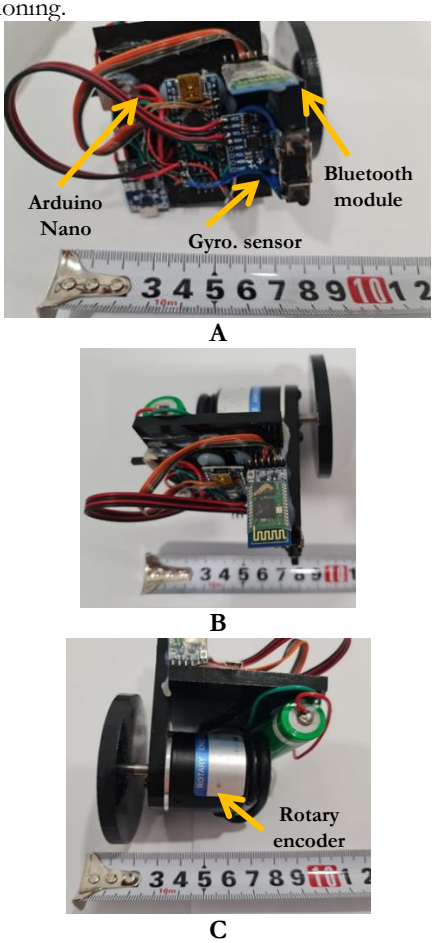

Figure (1): The main hardware components of the proposed system.

2.1.1. Angle Measurement

Euler angles are chosen as a simple and descriptive option among various approaches for describing

angles [29], which measure the rotation of an object from a reference point around a central axis. Sensors often quantify angles in a manner that can be comprehended, analyzed, and applied by a computer. Gyroscope sensors detect angular velocity as well as determine the object's motion. There are three types of angular rate measurements: Yaw for horizontal rotation viewed from above, Pitch for vertical rotation observed from the front, and Roll for horizontal rotation viewed from the front, as shown in Fig. 2. Gyroscope sensors utilize the Coriolis force idea. This sensor measures the angular rate by converting the rotation rate of the sensor into an electrical signal [30]. The proposed system neglects the Yaw angle because the z-axis, parallel to the yaw axis of reference, is unaffected by gravitational pull. The arctangent of the ACC data can be utilized to calculate the Euler angles [29]:

$$[Pitch(\theta) = \text{atan}\left(\frac{ACCx}{\sqrt{(ACCy^2+ACCz^2)}}\right) \times [\left(\frac{180}{\pi}\right)] \quad \ldots(1)$$

$$Roll(\phi) = \text{atan}\left(\frac{ACCy}{\sqrt{(ACCx^2+ACCz^2)}}\right) \times \left(\frac{180}{\pi}\right)] \quad \ldots(2)$$

Where:
ACCx: Acceleration in the x-axis.; ACCy: Acceleration in the y- axis; ACCz: Acceleration in the z- axis.

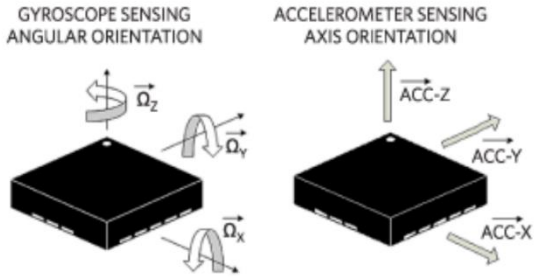

Figure (2): Gyro's roll, pitch, and yaw orientations [28].

The gyroscope sensor signal was filtered in real-time on the Arduino Nano microcontroller using the moving average filter. A process of iterative experimentation achieves optimal window size selection. In this design, a window size of 10 samples was chosen to implement a moving average filter on the Arduino Nano microcontroller. The purpose of this filter is to remove the time delay between the filter's input and output signals [27]. The data is processed to attenuate high-frequency interference prior to transmission to a computer via a Bluetooth module.

2.1.2. Distance Measurement

The working principle of the incremental encoder is that the aperture allows light to pass through to a photodiode on one side of the disk. A photodetector on the other side of the disk detects the light beam. The photodiode generates a waveform that is directly related to the intensity of the incoming light and has a nearly sinusoidal shape. A Schmitt Trigger is used to take the sinusoidal waveform and square it, as shown in Fig. 3 [28]. An incremental encoder consists of uniformly spaced slits arranged in a pattern (line or band of slits) around the disc's perimeter. The encoder resolution, denoted as Ŕ, is measured in pulses per revolution (PPR) and can be multiplied by a factor y (where y might be 1, 2, or 4) based on the encoder peripheral setup. The number of slits positioned around the whole 360 degrees determines the resolution of the encoder. The resolution is the smallest unit of rotation, denoted as θ, that can be detected. The encoder resolution is determined in degrees and denoted as:

$$[\theta = \frac{360^\circ}{\acute{R}.y}] \quad \ldots(3)$$

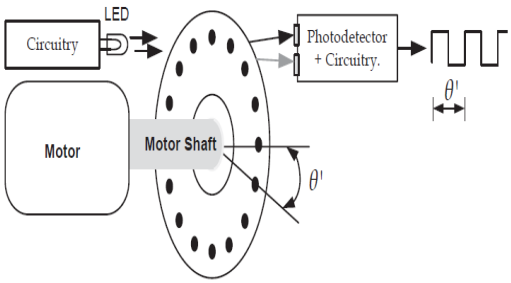

Figure (3): The working principle of the incremental encoder [28]

Fig. 4a illustrates how an incremental optical encoder indicates the immediate position of a rotating shaft by generating two output square wave cycles for each increment of shaft movement. The two output waveforms, called quadrature signals, are 90 degrees out of phase [31].

Fig. 4b shows digital quadrature signals generating channels A and B. y = 1 if only a single channel's rising or falling edges are being measured. When considering both the rising and falling edges of a single channel, y equals 2. If the rising and falling edges of both Channel A and Channel B are employed, y equals 4, which is generally referred to as the quadrature configuration mode. The sensor's quadrature arrangement enables the detection of rotation direction by analyzing the relative phasing of the two channels [32].

To calibrate the encoder and determine the distance, a mark was placed on the wheel with a diameter of 60 mm. The wheel was then passed over a ruler and moved by 800 pulses, corresponding to a complete revolution. The encoder travelled a distance of 23 cm, which was then translated to millimetres. The value of 230 mm was divided into 800 pulses, resulting in a ratio of 0.2875. The number of pulses generated during the encoder rotation on the patient's back is multiplied by 0.2875 and then converted to millimetres. Consequently, the distance has been measured in millimetres instead of pulses.

Fig. 5 illustrates the final design of the proposed system. The main driving force behind the development was the lack of a method or technology that could assess the structure and flexibility of the spinal column without being invasive or involving radiation. The goal was to find a solution that was simple, fast, reliable, and cost-effective.

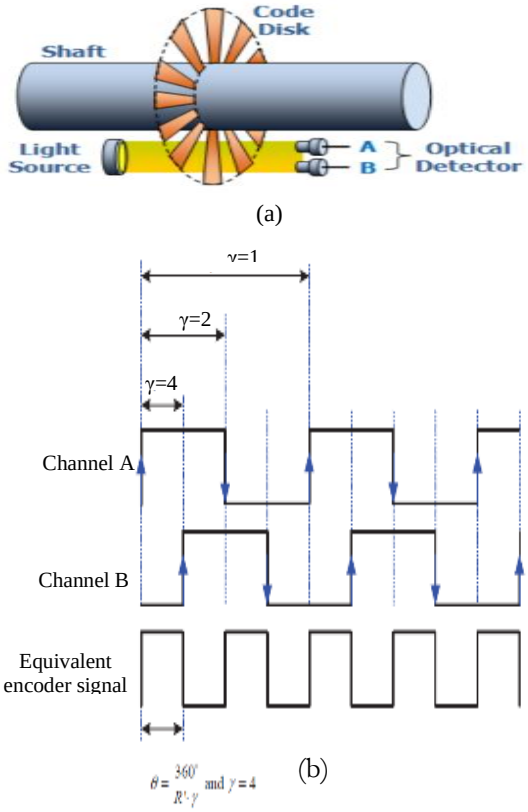

Figure (4): Varying encoder setups with digitally enhanced resolution [31, 32].

Figure (5): The proposed system (SM).

2.2. Participants

The study group was comprised of five adult healthy volunteers who agreed to participate in the study, aged between 25 and 50 years old, and who had no previous back problems. The mean age of the participants was 37.5 years, with a mean height of 1.77 meters, mean weight of 75.6 kilograms, and mean BMI of 25.95 kg/m^2, as shown in Table 1. None had any low back pain at the time of testing or had done so within the preceding two weeks. The volunteers gave signed, informed consent to participate. The study was conducted at Ramadi Teaching Hospital in the city of Ramadi, Anbar Governorate.

2.3. Measurement Protocol

The proposed methodology employs the SM, a computer-assisted, non-invasive apparatus, to evaluate sagittal spinal alignment. Five healthy individuals were subjected to measurements by three distinct physiotherapists on the same day. Participants were instructed to assume a relaxed stance by positioning their arms across their body and standing symmetrically, distributing their weight evenly between both feet to the best of their ability. Measurements were conducted in three distinct trunk positions: upright, maximum flexion, and maximum extension. They were carried out 1 to 2 minutes apart. During an upright posture, the participant was instructed to maintain a comfortable stance, facing horizontally towards the wall, with their feet shoulder-width apart. They were also ordered to keep their knees straight and arms by their sides. During maximal flexion, the participant was asked to bend the back while keeping their legs straight, attempting to touch the ground with their fingertips. During the maximal extension phase, the participant was asked to cross one arm over the other, place them on the chest and extend their trunk as much as possible while keeping their cervical spine (neck) upright without any extension. The device travelled along the spine's central axis, beginning at the spinous process of C7 and ending at S3. Afterwards, the spinous processes of C7 and S3 were marked using a non-irritating cosmetic pencil, as shown in Fig. 7.

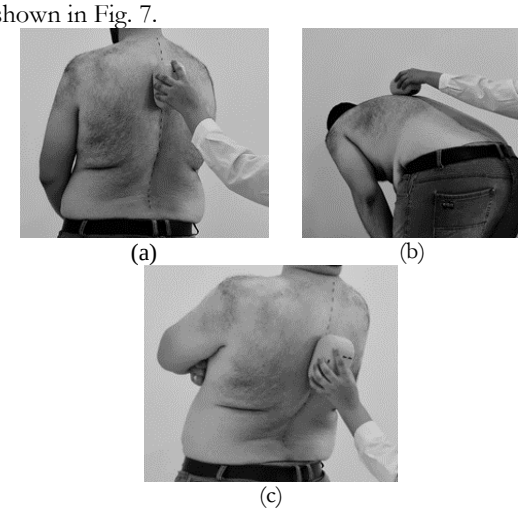

Figure (6): Measurement Protocol, (a) Upright, (b) Flexion, and (c) Extension.

The SM measured the following variables: thoracic kyphosis angle (the sum of 11 segmental angles from Th1/2 to Th11/12); lumbar lordosis angle (the sum of 6 segmental angles from Th12/L1 to L5/S1). After taking measurements in the three positions of the volunteer by the first examiner, the volunteer goes to the second examiner, and the skin marks are remained the same and measurements are taken by the second examiner and then repeated again by the third examiner, and carry out the same three sets of measures. Each physiotherapist repeated the measurements thrice, and the average value was utilized for analysis. Subsequently, the data was communicated wirelessly to a personal computer using Bluetooth technology, and subsequently, the data was presented and examined using software programming.

2.4. Statistical analysis

The statistical analysis was conducted using IBM SPSS version 21. The inter-rater and intra-rater reliability of the back's length and angle in flexion, extension, and thoracic segment and lumbar segment was assessed using the ICC with corresponding 95% confidence intervals. The inter-rater reliability—ICC(2,k) 2-way-random, average measure (k = 3 examiners)— represents the difference among two or more examiners who assess the same set of individuals, while intra-rater reliability—ICC(2,1) 2-way random, single measure—represents the range of data

measured by one evaluator across two or more attempts. The ICC values vary from 0 to 1, with a higher value indicating more excellent dependability. These numbers are used to assess the level of reliability according to the following basic guidelines: values below 0.5 suggest low dependability, values between 0.5 and 0.75 suggest moderate reliability, values between 0.75 and 0.9 suggest high reliability, and values over 0.90 suggest exceptional reliability [33].

3. Results

The suggested SM conducted tests on five healthy adult volunteers. Three examiners conducted measurements for each volunteer, and the resulting parameters that define sagittal spinal alignment are displayed in Table 1. The first examiner, who had eight years of expertise as a physical therapist specializing in orthopaedic examination and therapy, took measurements for one volunteer. The measurements were summarized in three columns. These columns represent the values for standing posture in the following order: upright, flexion, and extension. Positive values indicate kyphotic angles, while negative values indicate lordotic angles. The proposed SM was utilized to measure the variable factors, precisely the angle between the two vertebrae from (T1-T2) to (T12-L1) and from (L1-L2) to (L5-S1). Additionally, the sum of the angle of the thoracic section, the sum of the angle of the lumbar section, and the length of the spine in millimetres were computed. The results were within the reference values for the standing sagittal posture (18-83 years) [34] in the thoracic and lumber segments.

Table (1): The initial examiner recorded the volunteer's measures. The data is saved and provided by the software of the SM in degrees. Data refers to the angles measured in three positions: thoracic segment (Thor. Seg), lumbar segment (Lum. Seg), and the length of the spine in millimeters (Lth). Kyphotic values are positive, whereas lordotic values are negative.

Segment	Upright	Flexion	Extension
Th1/2 (°)	1.40	1.12	2.45
Th2/3 (°)	1.78	2.50	3.87
Th3/4 (°)	2.51	3.81	2.10
Th4/5 (°)	3.42	3.58	3.91
Th5/6 (°)	2.56	3.32	3.96
Th6/7 (°)	3.43	5.18	2.19
Th7/8 (°)	3.85	5.79	2.49
Th8/9 (°)	2.33	4.73	3.73
Th9/10 (°)	1.61	3.80	-0.67
Th10/11 (°)	-1.54	5.99	-3.50
Th11/12 (°)	-0.99	2.17	-5.82
Th12/L1 (°)	-2.50	2.34	-7.42
L1/2 (°)	-5.59	5.26	-6.04
L2/3 (°)	-8.93	2.36	-5.24
L3/4 (°)	-8.02	2.76	-10.00
L4/5 (°)	-8.11	4.07	-8.50
L5/S1 (°)	-11	3.13	-5.33
Thor. Seg (°)	17.95	44.33	7.29
Lum. Seg (°)	-41.65	17.58	-35.11
Lth (mm)	501	578	465

The bar chart in each upright, flexion, and extension position displays the difference between the reference values and the measured values; this indicates that the results of the two sets of measurements are converging, as illustrated in Figs. 7, 8, and 9.

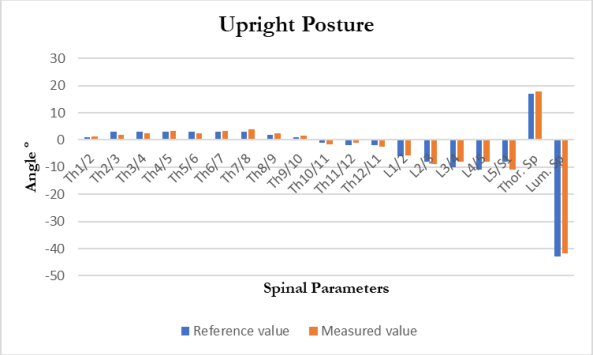

Figure (7): Reference VS. Measured in Upright posture.

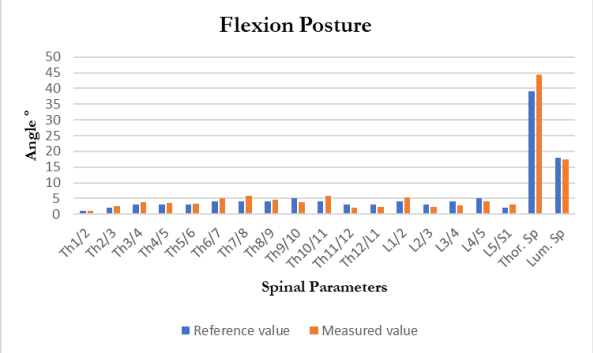

Figure (8): Reference VS. Measured in Flexion posture.

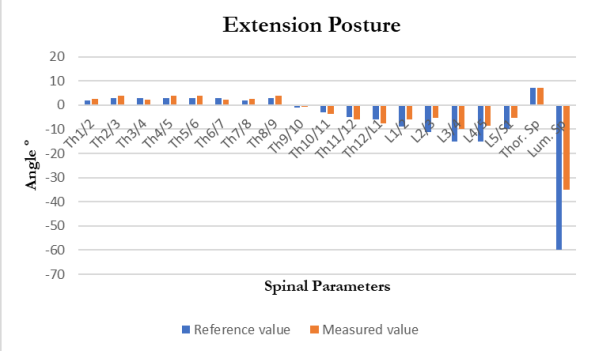

Figure (9): Reference VS. Measured in Extension posture.

Table 2 displays the mean measures of five participants taken by the first examiner. He assessed each participant separately using a non-irritating cosmetic pencil to identify the vertebrae. The measured values exhibited a high degree of reliability across all participants.

Table (2): Intra-examiner reliability (examiner versus himself on five volunteers).

Segment	Upright	Flexion	Extension
Th1/2 (°)	1.243	1.042	2.012
Th2/3 (°)	3.094	2.004	3.039
Th3/4 (°)	3.138	3.025	3.015
Th4/5 (°)	3.100	3.099	2.986
Th5/6 (°)	2.902	2.979	2.889
Th6/7 (°)	2.960	4.113	2.996
Th7/8 (°)	3.152	4.039	2.098

Th8/9 (°)	2.253	4.023	3.133
Th9/10 (°)	1.098	4.967	-1.098
Th10/11 (°)	-1.268	4.089	-3.021
Th11/12 (°)	-2.078	3.110	-5.022
Th12/L1 (°)	-2.223	3.012	-6.132
L1/2 (°)	-5.970	4.036	-9.014
L2/3 (°)	-8.052	3.009	-10.994
L3/4 (°)	-9.958	4.036	-15.100
L4/5 (°)	-10.964	5.099	-14.970
L5/S1 (°)	-8.106	2.132	-9.991
Thor. Seg (°)	17.371	40.393	6.895
Lum. Seg (°)	-43.05	18.312	-60.195
Lth (mm)	499	555	435

To demonstrate the effectiveness of the suggested device, the first participant underwent examination by three examiners. The first examiner had a total of 8 years of expertise in the field of physical therapy. The examiner used a cosmetic pencil to indicate the vertebrae on the skin of the initial participant and obtained measurements in three different positions (flexed, extended, and neutral) in the sagittal plane. Subsequently, the examiner, who had one year of experience and was part of the same volunteer group, repeated the same procedures using the same markers on the volunteer's skin. The third examiner, a student specializing in physical therapy, also performed the same procedure again.

Table 3 displays the ICC for the segmental and global thoracic and lumbar values obtained by three examiners with th volunteer. The measurements did not show any notable disparities in the values of the parameters examined, as indicated in Table 3. The ICC for the thoracic segment in the upright position was 0.947, with a range of 0.621 to 0.877. For the lumbar segment, the ICC was 0.969, with a range of 0.727 to 0.936. The ICC for the thoracic segment in the flexion position was 0.879 (with a range of 0.667 to 0.904), and for the lumbar segment, it was 0.977 (with a range of 0.639 to 0.843). Finally, in the extended position, the ICC for the thoracic segment was 0.960 (with a range between 0.752 and 0.859), and for the lumbar segment, it was 0.706 (with a range between 0.656 and 0.752).

Table (3): The interrater reliability (ICC) of the segmental thoracic and lumbar values in three positions.

Segment	ICC		
	Upright	Flexion	Extension
Global thoracic	0.94	0.87	0.96
Th1/2	0.71	0.89	0.81
Th2/3	0.71	0.80	0.77
Th3/4	0.85	0.78	0.73
Th4/5	0.87	0.83	0.76
Th5/6	0.87	0.90	0.75
Th6/7	0.87	0.77	0.78
Th7/8	0.77	0.69	0.80
Th8/9	0.85	0.84	0.82
Th9/10	0.62	0.80	0.75
Th10/11	0.64	0.66	0.85
Th11/12	0.66	0.78	0.86
Th12/L1	0.80	0.81	0.80
Global lumber	0.96	0.97	0.70
L1/2	0.93	0.76	0.75
L2/3	0.89	0.82	0.65
L3/4	0.83	0.76	0.75
L4/5	0.79	0.84	0.69
L5/S1	0.72	0.63	0.68

4. Discussion

This study aimed to design and fabricate a tool to assess the spinal curvature as well as provide a visual representation of the spinal alignments and enable accurate estimation of clinical indexes of spine deformities. The investigation was conducted on healthy adult volunteers at Ramadi Teaching Hospital in Ramadi, Anbar Governorate. In the present study, the angles of the thoracic and lumbar segments, as well as the length of the spine, were measured with the suggested device, as shown in Table (1). The results closely approximated the reference values for the SM device [34], in Fig. 7, 8, and 9, the bar chart in each upright, flexion, and extension position displays the difference between the reference values and the measured values. In general, the measurement of global thoracic and lumbar using the proposed device showed a high level of reliability among participants, with interrater reliability ranging from 0.621 to 0.936. The evaluation of the degree of flexing in the individual sections of the spine, specifically the thoracic and lumbar regions, resulted in a high level of agreement across different examiners about the trustworthiness of these measurements. The ICC value for the lumber region in the extension position is 0.706, which is good. However, examiners have encountered many cases where the suggested SM device was missing in maintaining complete contact with the lumbar spine of volunteers with excessive lumbar lordosis in the extension position, which may be related to the low global lumbar extension reliability values. The irregular contact of the proposed device on the volunteer's spine might have caused measurement mistakes, influencing the reliability scores, despite the fact that motion evaluation was done as precisely as feasible in these cases. The high global intra-rater and inter-rater reliability may have been caused by the fact that each examiner utilized the same skin markings for their evaluations. A study discovered that the reliability of mobility assessments was significantly higher when the same skin markings were used, as opposed to when each examiner independently applied the skin markings [25].

In this study, a threshold of 0.70 and above was considered acceptable, indicating that the inter-rater reliability was satisfactory for all volunteers, even for the level of L1-L2 to L5-S1.

To assess the device's ability to evaluate sagittal spinal alignment, one may have compared the data generated from the proposed SM with radiography. The use of radiography is probably unjustified, given the potential hazards to patients and the related costs, especially when assessing the complete spinal column. However, to obtain a more accurate spine diagnostic before surgery or select the most effective treatment plan, it is ideal to apply radiological instruments.

Conversely, the proposed SM has been evaluated as a follow-up of the patient's clinical state, specifically to gather fundamental data regarding the curvature and alignment of the spine, which can indicate their

overall health condition. The device presented in this study is user-friendly and requires no extensive training. The examiner only needs to spend less than one hour before the examination to acquire the necessary knowledge and skills on how to utilize it and the methods of measurement; each measurement necessitates around 1 minute to be completed. The gadget is unaffected by velocity, and the SM becomes highly manageable with sufficient training.

5. Limitations

Some limitations are associated with this study, with the most significant being that the examiners took measurements of backward extent, mainly when the participant was tested multiple times. A discrepancy in the reading occurred due to the volunteer's unbalanced and uncomfortable position. Furthermore, when flexing forward, the mark applied on the skin to identify the position of the vertebrae extends and reaches the neighbouring vertebra, resulting in a reading error. Furthermore, the examiner's expertise is necessary to identify vertebrae from C7 to S1.

6. Conclusion

The suggested SM equipment demonstrated satisfactory intra-rater and inter-rater reliability when used to assess overall sagittal spinal alignment in the thoracic and lumbar regions of five healthy adult volunteers. Moreover, the use of this equipment for segmental lumbar extension measurements showed satisfactory reproducibility between the examiners.

The proposed system is an effective and dependable instrument for assessing sagittal spinal alignment. The gyroscope sensor offered accurate measurements of the angle between two vertebrae and the angle of the thoracic and lumbar segments, ensuring precision in the system's outcomes. Moreover, the rotary encoder sensor can be used to determine the exact spinal length and the specific position of the vertebrae. In general, the proposed SM demonstrated consistent agreement across several evaluators when assessing the curvatures and deformations of the spine, as well as the body's position in the sagittal plane; this is attributed to its efficient clinical measurement duration and minimal health risks to the patient.

The proposed device could be improved to measure spinal deformity in the sagittal and frontal planes in upright, lateral to the right, and lateral to the left positions, as well as the range of motion. The device would give enough variables to reliably identify the spine's straightness and mobility, allowing for a radiation-free diagnostic. It is possible to improve the recommended device software to allow data transmission and upload from anywhere.

7. References:

[1] V. Mahadevan, "Anatomy of the vertebral column," *Surgery (Oxford),* vol. 36, no. 7, pp. 327-332, 2018.

[2] P. J. Bazira, "Clinically applied anatomy of the vertebral column," *Surgery (Oxford),* vol. 39, no. 6, pp. 315-323, 2021.

[3] S. Mihcin, "Spinal curvature for the assessment of spinal stability," *International Journal of Biomedical Engineering and Technology,* vol. 20, no. 3, pp. 226-242, 2016.

[4] J.-O. Yoon, M.-H. Kang, J.-S. Kim, and J.-S. Oh, "The effects of gait with use of smartphone on repositioning error and curvature of the lumbar spine," *Journal of physical therapy science,* vol. 27, no. 8, pp. 2507-2508, 2015.

[5] M. Masaki, T. Ikezoe, Y. Fukumoto, S. Minami, J. Aoyama, S. Ibuki, M. Kimura, and N. Ichihashi, "Association of walking speed with sagittal spinal alignment, muscle thickness, and echo intensity of lumbar back muscles in middle-aged and elderly women," *Aging clinical and experimental research,* vol. 28, pp. 429-434, 2016.

[6] S. M. Walaa and M. E. Walaa, "Prevalence of scoliosis among Majmaah University physical therapy students-Saudi Arabia," *International Journal of Medical Research & Health Sciences,* vol. 5, no. 10, pp. 187-191, 2018.

[7] K. Sugai, T. Michikawa, T. Takebayashi, M. Matsumoto, M. Nakamura, and Y. Nishiwaki, "Association between visual classification of kyphosis and future ADL decline in community-dwelling elderly people: the Kurabuchi study," *Archives of Osteoporosis,* vol. 14, pp. 1-9, 2019.

[8] N. Azevedo, J. C. Ribeiro, and L. Machado, "Balance and Posture in Children and Adolescents: A Cross-Sectional Study," *Sensors,* vol. 22, no. 13, p. 4973, 2022.

[9] A. Cepková, E. Zemková, Ľ. Šooš, M. Uvaček, and J. M. Muyor, "Sedentary lifestyle of university students is detrimental to the thoracic spine in men and to the lumbar spine in women," *PloS one,* vol. 18, no. 12, p. e0288553, 2023.

[10] M. S. Shehada, N. Karimi, P. Baraghoosh, F. Mohammadi, and A. Ahmadi, "Prevalence and Factors Associated With Postural Abnormalities in Male Students of Tehran Universities: A Cross-sectional Study," فیزیک درمانی-نشریه تخصصی فیزیوتراپی, vol. 13, no. 2, pp. 0-0, 2023.

[11] N. Azevedo, J. C. Ribeiro, and L. Machado, "Back pain in children and adolescents: a cross-sectional study," *European Spine Journal,* pp. 1-10, 2023.

[12] V. Zaborova, O. Zolnikova, N. Dzhakhaya, S. Prokhorova, A. Izotov, T. Butkova, V. Pustovoyt, K. Yurku, D. Shestakov, and T. Zaytseva, "Associations between Physical Activity and Kyphosis and Lumbar Lordosis Abnormalities, Pain, and Quality of Life in Healthy Older Adults: A Cross-Sectional Study," in *Healthcare*, 2023, vol. 11, no. 19: MDPI, p. 2651.

[13] Ş. T. Çelenay and D. Ö. Kaya, "Relationship of spinal curvature, mobility, and low back pain in womenwith and without urinary incontinence," *Turkish journal of medical sciences,* vol. 47, no. 4, pp. 1257-1262, 2017.

[14] A. Muramoto, S. Imagama, Z. Ito, K. Hirano, N. Ishiguro, and Y. Hasegawa, "Spinal sagittal balance substantially influences locomotive syndrome and physical performance in community-living middle-aged and elderly

women," *Journal of Orthopaedic Science,* vol. 21, no. 2, pp. 216-221, 2016.

[15] M. Machino, K. Ando, K. Kobayashi, H. Nakashima, S. Kanbara, S. Ito, T. Inoue, H. Yamaguchi, H. Koshimizu, and T. Seki, "Influence of global spine sagittal balance and spinal degenerative changes on locomotive syndrome risk in a middle-age and elderly community-living population, BioMed Research International, vol. 2020, 2020," *DOI: https://doi.org/10.1155/2020/3274864*.

[16] R. Corona-Cedillo, M.-T. Saavedra-Navarrete, J.-J. Espinoza-Garcia, A.-N. Mendoza-Aguilar, S. K. Ternovoy, and E. Roldan-Valadez, "Imaging assessment of the postoperative spine: an updated pictorial review of selected complications," *BioMed Research International,* vol. 2021, pp. 1-20, 2021.

[17] M. S. Linet, T. L. Slovis, D. L. Miller, R. Kleinerman, C. Lee, P. Rajaraman, and A. Berrington de Gonzalez, "Cancer risks associated with external radiation from diagnostic imaging procedures," *CA: a cancer journal for clinicians,* vol. 62, no. 2, pp. 75-100, 2012.

[18] E. E. Rutherford, L. J. Tarplett, E. M. Davies, J. M. Harley, and L. J. King, "Lumbar spine fusion and stabilization: hardware, techniques, and imaging appearances," *Radiographics,* vol. 27, no. 6, pp. 1737-1749, 2007.

[19] S. Zamani, F. Okhovatian, S.-S. Naemi, and A. A. Baghban, "Intra-examiner reliability of goniometer instrument for all active movements of cervical spine in asymptomatic young women," *J Rehab Med,* vol. 4, no. 4, pp. 57-64, 2016.

[20] C. M. Todd, C. Agnvall, P. Kovac, A. Sward, C. Johansoon, L. Sward, J. Karlsson, and A. Baranto, "Validation of spinal sagittal alignment with plain radiographs and the Debrunner Kyphometer," *Medical Research Archives,* vol. 2, no. 1, 2015.

[21] M. Adams, P. Dolan, C. Marx, and W. Hutton, "An electronic inclinometer technique for measuring lumbar curvature," *Clinical Biomechanics,* vol. 1, no. 3, pp. 130-134, 1986.

[22] A. Topalidou, G. Tzagarakis, K. Balalis, and A. Papaioannou, "Posterior decompression and fusion: whole-spine functional and clinical outcomes," *PloS one,* vol. 11, no. 8, p. e0160213, 2016.

[23] I. A. O. M. T. PtyLtd. "Idiag M360." Idiag https://idiagm360.com.au/idiag/ (accessed.

[24] R. B. Post, C. K. van der Sluis, V. Leferink, and H.-J. ten Duis, "Long-term functional outcome after type A3 spinal fractures: operative versus non-operative treatment," *Acta orthopaedica belgica,* vol. 75, no. 3, p. 389, 2009.

[25] A. F. Mannion, K. Knecht, G. Balaban, J. Dvorak, and D. Grob, "A new skin-surface device for measuring the curvature and global and segmental ranges of motion of the spine: reliability of measurements and comparison with data reviewed from the literature," *European Spine Journal,* vol. 13, pp. 122-136, 2004.

[26] J. Zafereo, S. Wang-Price, J. Brown, and E. Carson, "Reliability and comparison of spinal end-range motion assessment using a skin-surface device in participants with and without low back pain," *Journal of manipulative and physiological therapeutics,* vol. 39, no. 6, pp. 434-442, 2016.

[27] K. Nirmal, A. Sreejith, J. Mathew, M. Sarpotdar, A. Suresh, A. Prakash, M. Safonova, and J. Murthy, "Noise modeling and analysis of an IMU-based attitude sensor: improvement of performance by filtering and sensor fusion," in *Advances in optical and mechanical technologies for telescopes and instrumentation II*, 2016, vol. 9912: SPIE, pp. 2138-2147.

[28] Y. Vazquez-Gutierrez, "Contributions to the modeling of the incremental optical encoder and speed estimation methods for motion control," 2019.

[29] C. K. Mummadi, F. Philips Peter Leo, K. Deep Verma, S. Kasireddy, P. M. Scholl, J. Kempfle, and K. Van Laerhoven, "Real-time and embedded detection of hand gestures with an IMU-based glove," in *Informatics*, 2018, vol. 5, no. 2: MDPI, p. 28.

[30] B. R. Chandra, "Development of Gyroscopic Angle Measuring Sensor by Using Arduino," 2022.

[31] M. Afandi, H. Adinanta, A. Setiono, and B. Widiyatmoko, "High resolution extensometer based on optical encoder for measurement of small landslide displacements," in *Journal of Physics: Conference Series*, 2018, vol. 985, no. 1: IOP Publishing, p. 012007.

[32] Y. Vazquez-Gutierrez, D. L. O'Sullivan, and R. C. Kavanagh, "Evaluation of three optical-encoder-based speed estimation methods for motion control," *The Journal of Engineering,* vol. 2019, no. 17, pp. 4069-4073, 2019.

[33] T. K. Koo and M. Y. Li, "A guideline of selecting and reporting intraclass correlation coefficients for reliability research," *Journal of chiropractic medicine,* vol. 15, no. 2, pp. 155-163, 2016.

[34] *xUser_Guide_SM*, 2013. [Online]. Available: https://static1.squarespace.com/static/51763de2e4b0e95e599b4f29/t/52fceaa5e4b01b2bb4f8caba/1392306853736/xUser_Guide_SM_SW_EN_16.10.13.pdf.